Self-organization of bacterial biofilms is facilitated by extracellular DNA

Erin S. Gloag[a,1], Lynne Turnbull[a,1], Alan Huang[b], Pascal Vallotton[c], Huabin Wang[d], Laura M. Nolan[a], Lisa Mililli[e], Cameron Hunt[e], Jing Lu[a], Sarah R. Osvath[a], Leigh G. Monahan[a], Rosalia Cavaliere[a], Ian G. Charles[a], Matt P. Wand[b], Michelle L. Gee[d], Ranganathan Prabhakar[e], and Cynthia B. Whitchurch[a,2]

[a]The ithree institute and [b]School of Mathematical Sciences, University of Technology Sydney, Ultimo, NSW 2007, Australia; [c]Mathematics, Informatics, and Statistics, Commonwealth Scientific and Industrial Research Organization, North Ryde, NSW 1670, Australia; [d]School of Chemistry, University of Melbourne, Parkville, VIC 3010, Australia; and [e]Department of Mechanical and Aerospace Engineering, Monash University, Clayton, VIC 3800, Australia

Edited by Caroline S. Harwood, University of Washington, Seattle, WA, and approved May 21, 2013 (received for review November 1, 2012)

Twitching motility-mediated biofilm expansion is a complex, multicellular behavior that enables the active colonization of surfaces by many species of bacteria. In this study we have explored the emergence of intricate network patterns of interconnected trails that form in actively expanding biofilms of *Pseudomonas aeruginosa*. We have used high-resolution, phase-contrast time-lapse microscopy and developed sophisticated computer vision algorithms to track and analyze individual cell movements during expansion of *P. aeruginosa* biofilms. We have also used atomic force microscopy to examine the topography of the substrate underneath the expanding biofilm. Our analyses reveal that at the leading edge of the biofilm, highly coherent groups of bacteria migrate across the surface of the semisolid media and in doing so create furrows along which following cells preferentially migrate. This leads to the emergence of a network of trails that guide mass transit toward the leading edges of the biofilm. We have also determined that extracellular DNA (eDNA) facilitates efficient traffic flow throughout the furrow network by maintaining coherent cell alignments, thereby avoiding traffic jams and ensuring an efficient supply of cells to the migrating front. Our analyses reveal that eDNA also coordinates the movements of cells in the leading edge vanguard rafts and is required for the assembly of cells into the "bulldozer" aggregates that forge the interconnecting furrows. Our observations have revealed that large-scale self-organization of cells in actively expanding biofilms of *P. aeruginosa* occurs through construction of an intricate network of furrows that is facilitated by eDNA.

collective behavior | t4p | type IV pili | tfp | swarming

Bacterial biofilms are multicellular communities of bacteria that are embedded in a self-produced polymeric matrix comprised of polysaccharides, proteins, and extracellular DNA (eDNA). Biofilms are prevalent in nature as well as in industrial and medical settings, where colonization of new territories by bacteria can occur via active biofilm expansion, leading to biofouling of marine and industrial surfaces, and the spread of infection within host tissues and along implanted medical devices (1–3).

When cultured on the surface of solidified nutrient media, many bacteria are able to actively expand their colony biofilms through coordinated motions that can be powered by different mechanisms including flagella rotation, type IV pili (tfp) retraction, and/or slime secretion. The soil organism *Myxococcus xanthus* actively swarms away from the point of inoculation through a process termed gliding motility, which is mediated by two types of motility: A motility that occurs through an unknown mechanism, and S motility, which is powered by tfp retraction (4, 5). *M. xanthus* swarming is a complex multicellular process that has been extensively studied, and in recent years a number of mathematical models have been developed to describe this behavior (6–9).

Twitching motility is a mechanism of surface translocation that has been observed in many species of bacteria (10) and is closely related to S motility of *M. xanthus*. Both of these motilities are powered by the extension, surface binding, and retraction of tfp located at the leading edge pole of the cell, resulting in translocation of an individual bacterial cell (11, 12). We have observed previously that when the opportunistic pathogen *Pseudomonas aeruginosa* is cultured at the interface of solidified nutrient media and a glass coverslip, the biofilms that form in the interstitial space expand rapidly via twitching motility and can form a vast, intricate network of interconnected trails (13). Interstitial biofilm expansion by *P. aeruginosa* appears to be a highly organized multicellular behavior that arises through the collective coordination of individual cellular movements involving the migration of rafts of cells at the leading edge of the biofilm that appear to lay down a trail of unknown composition along which cells preferentially migrate (13). The mechanisms involved in coordinating individual activities during this complex multicellular behavior or that lead to the formation of the dramatic interconnected trail network in *P. aeruginosa* biofilms are currently unknown.

The emergence of self-organized patterns in living and nonliving systems has fascinated scientists for centuries, and there is widespread interest in understanding the mechanisms behind these (14). Common features displayed by these self-organized phenomena are the formation of trails that lead to the emergence of dramatic patterns of large-scale order (15). The processes leading to pattern formation in biological systems are likely to be more complex than the spontaneous emergence of patterns that are observed in nonliving systems and will involve an interplay of physical, chemical, and biological parameters (16, 17).

Multicellular behaviors in bacteria are often controlled via chemical signaling systems such as quorum sensing (18). However, we have shown previously that twitching motility–mediated biofilm expansion by *P. aeruginosa* is not controlled through quorum sensing (19). Interestingly, the exopolysaccharide slimes that are produced during gliding and flagella-dependent swarming motilities are visualized microscopically as phase-bright trails. These slime trails are laid down by cells as they migrate across the surface and direct cellular movements of following cells (20, 21). In *M. xanthus*, tfp have also been shown to bind to the polysaccharide component of extracellular fibrils located on the surface of neighboring cells. The production of fibrils is essential for S motility in *M. xanthus*, where it is thought that the polysaccharide component provides an optimal surface for tfp binding, inducing

Author contributions: E.S.G., L.T., M.L.G., and C.B.W. designed research; E.S.G., L.T., H.W., L.M.N., S.R.O., L.G.M., R.C., and C.B.W. performed research; A.H., P.V., L.M., C.H., J.L., M.P.W., and R.P. contributed new reagents/analytic tools; E.S.G., L.T., A.H., P.V., H.W., L.M.N., I.G.C., M.P.W., M.L.G., R.P., and C.B.W. analyzed data; and E.S.G., L.T., P.V., R.P., and C.B.W. wrote the paper.

The authors declare no conflict of interest.

This article is a PNAS Direct Submission.

Freely available online through the PNAS open access option.

[1]E.S.G. and L.T. contributed equally to this work.

[2]To whom correspondence should be addressed. E-mail: cynthia.whitchurch@uts.edu.au.

This article contains supporting information online at www.pnas.org/lookup/suppl/doi:10.1073/pnas.1218898110/-/DCSupplemental.

retraction of the filament and subsequent translocation of the cell (22). It has not yet been determined if an extracellular slime similarly contributes to *P. aeruginosa* twitching motility–mediated biofilm expansion.

Results

Quantitative Analysis of Cell Movements During Interstitial Biofilm Expansion. We have developed a model system to study interstitial biofilm expansion by *P. aeruginosa*, in which the interstitial biofilm expands via twitching motility as a monolayer. This model enables visualization of individual cells in the biofilm using high-resolution phase-contrast microscopy, which avoids potential phototoxicity artifacts that can be associated with the use of fluorescence microscopy. Time-series of *P. aeruginosa* intersititial biofilm expansion were captured at one frame per 2 s. Visual inspection of 1,000-frame time-series (2,000 s) shows that biofilm expansion involves an almost constant streaming of cells that migrate from the main biofilm along the trail network into rafts of cells at the leading edge (Movie S1). Cells behind the leading edge are tightly aligned in narrow intersecting trails with the major cell axes oriented along the overall direction of the trail in which they were moving. Cells within these trails appear to be in relatively constant motion with the overall direction of movement toward the leading edge (Movie S1).

To enable quantitative analyses of individual cellular movements during biofilm expansion, we have developed an automated cell-tracking algorithm to identify and track the movements of all individual bacterial cells present in the field of view across consecutive frames (*SI Materials and Methods*) (23, 24). Whereas individual bacteria can be distinguished clearly by human vision in our interstitial biofilm images (Fig. 1 *A* and *C*, Fig. S1*A*), obtaining their precise outlines using computer vision is relatively challenging. We therefore developed sophisticated computer vision methods to identify and track individual bacteria (*SI Materials and Methods*) (23, 24).

Quantitative analysis of the data obtained from the cell tracking was used to examine the cell movements during 100 s of interstitial biofilm expansion by *P. aeruginosa* (Fig. 1 *A*–*D*). Cells were separated into three populations based on their location within the biofilm. Cells within the leading edge vanguard rafts are referred to as "raft head," cells within the trail immediately behind the raft as "raft trails," and cells within the trail network as "behind the leading edge" (Fig. 1 *A* and *C*). Our quantitative analyses indicate that cells within the raft head tend to be highly aligned along the longitudinal axis of the cell (orientational coherence) (Fig. S2*A*) and to move in the same direction as their neighbors (velocity coherence) (Fig. 2*A*). Cells in raft trails and behind the leading edge, however, have reduced orientation and velocity coherence with their neighbors, indicating that these cells tend to move more independently of their nearest neighbors (Fig. 2*A*, Fig. S2*A*).

Analysis of the distance traveled by individual cells in 100 s reveals that cells within the raft head, raft trails, and behind the leading edge travel at similar total distances with median values of 5.77, 5.93, and 5.86 μm, respectively (Fig. 2*B*). However, the net displacements of the cells in these regions showed median values of 4.70, 1.95, and 2.56 μm, respectively (Fig. 2*C*). These analyses indicate that cells within the raft head undergo few directional changes, whereas cells located within the raft trails and behind the leading edge show more frequent directional changes, which accounts for the reduced correlation between total and net distances traveled. Analyses of time decays of orientation and velocity direction autocorrelations confirm that cells in the raft head tend to maintain their orientation and direction of travel, whereas cells in the trails tend to change their orientation and direction of travel more frequently (Fig. 2*D*, Fig. S2*B*).

Our visual observations of extended (2,000 s) time-series suggest that there is a relatively constant stream of cells moving through the trails toward the leading edge. To explore this further, the distances traveled across 2-s intervals (frame to frame) were analyzed. These analyses reveal that in any given 2-s interval, ~55% of cells in the raft head, 50% within the raft trails, and 40% behind the leading edge traverse distances between 0.1 and 1.3 μm, with the majority of these motile cells traveling between 0.1 and 0.4 μm/2 s (Fig. S3*A*).

Interestingly, *M. xanthus* cells also frequently change the direction of motion during swarm expansion. Mathematical modeling of *M. xanthus* swarming has suggested that cellular reversals enable a steady supply of cells to the advancing edge of the swarm by preventing traffic jams that form as a result of cellular collisions (6, 7). We propose that the changes in direction of motion displayed by *P. aeruginosa* cells within the trail network could similarly enable efficient flow of cells through the biofilm to supply the advancing edge. Once at the outer edge, cells within the advancing raft heads maintain high velocity coherence with their neighbors and exhibit few directional changes as they colonize new territories.

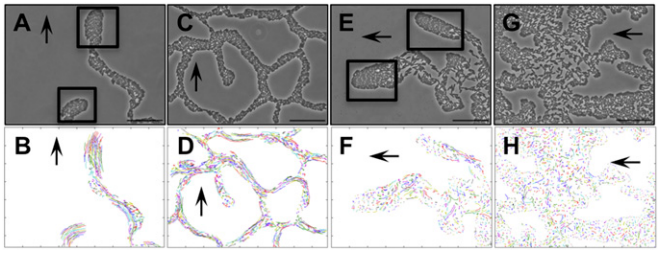

Fig. 1. Tracking of cellular movements during interstitial biofilm expansion. Time-series (one frame per 2 s) of interstitial biofilm expansion of *P. aeruginosa* strain PAK cultured on TMGG in the absence and presence of DNaseI (Movies S1 and S5). Regions at the leading edge of the expanding biofilms (*A* and *E*; Movies S1 and S5) and behind the leading edge (*C* and *G*; Movies S1 and S5) were imaged with phase-contrast microscopy. *A*, *C*, *E*, and *G* correspond to the first image of each time-series. (Scale bar, 20 μm.) Every cell present throughout the first 50 frames of each time-series was tracked and the paths traversed by each cell represented graphically (*B*, *D*, *F*, and *H*). Tick distance, 10 μm. Arrows indicate overall direction of movement away from the main biofilm toward unoccupied territory. Boxed regions (*A* and *E*) indicate cells in regions designated raft head, whereas the remainder of the cells in the field of view were designated as raft trails for the quantitative analyses of cell movements.

Twitching Motility–Mediated Biofilm Expansion Involves the Formation of a Network of Interconnected Furrows. Our observations indicate that during interstitial biofilm expansion, cells appear to be confined to trails of an unknown nature (Movie S1). We have found that similar to our observations of interstitial biofilm expansion, twitching motility–mediated expansion of the colony biofilm also involves the migration of aggregates of cells at the leading edge that venture into unoccupied territories. Interestingly, migration of these vanguard groups creates a phase-bright trail along which following cells are able to migrate individually or in small groups but remain confined to the trail (Fig. 3*A*, Movie S2). These phase-bright trails are very similar in appearance to the slime trails that are produced during gliding or flagella-dependent swarming motilities (20, 21). Indeed the edges of the expanding *P. aeruginosa* colony biofilms (Fig. 3*A*, Fig. S4*C*) bear a striking resemblance to *M. xanthus* swarms cultured on the surface of solidified growth media (25).

Our observations suggest that expansion of *P. aeruginosa* colony biofilms on the surface of solidified nutrient media is very similar to the expansion of interstitial biofilms. In light of the phase bright trails that we observed at the edges of the surface colony biofilms (Fig. 3*A*), we hypothesized that a similar trail

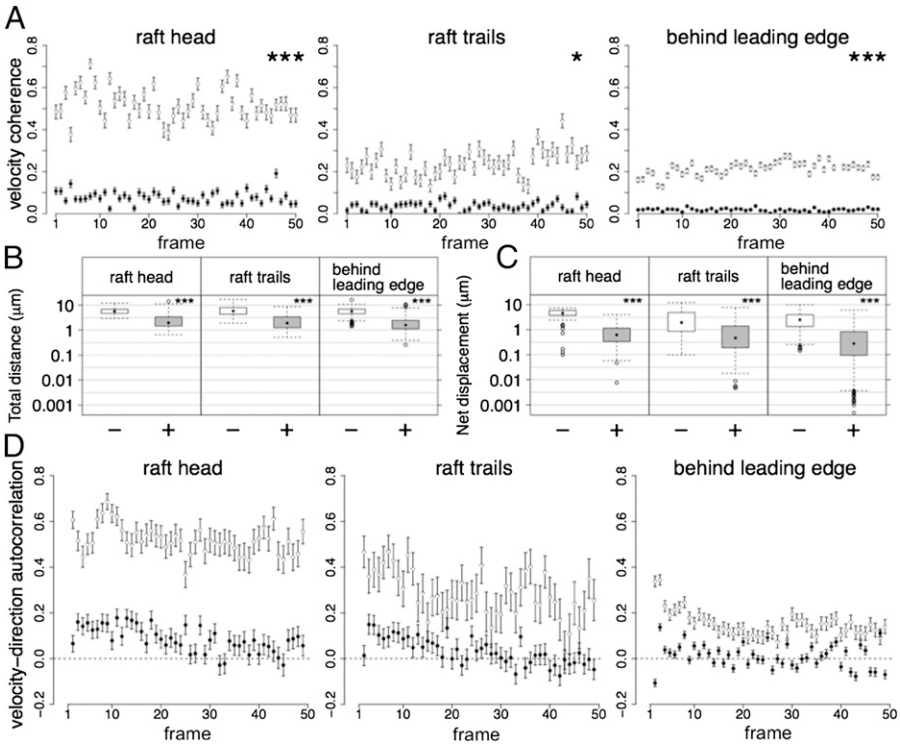

Fig. 2. Quantitative analyses of cell tracking data. (*A*) Velocity coherence across 50 frames of each cell with its closest neighbors in the indicated regions of the biofilm in the absence (○) and presence (●) of DNaseI. Each point indicates mean velocity coherence for all cells in a given frame. Error bars are ±SEM. Total distances (*B*) and net displacements (*C*) over 100 s of individual cells in the indicated regions of interstitial biofilms grown in the absence (–, white box) and presence (+, gray box) of DNaseI. (*D*) Autocorrelations of velocity direction in the indicated regions of the biofilm in the absence (○) and presence (●) of DNaseI. Each point indicates mean velocity direction autocorrelations for all cells in a given frame. Error bars are ±SEM. $^{***}P < 0.001$, $^{**}P < 0.01$, and $^{*}P < 0.05$ for comparisons of datasets obtained in the absence of DNaseI with corresponding datasets obtained in the presence of DNaseI.

network may exist within interstitial biofilms. To explore this possibility, the media that supported the *P. aeruginosa* interstitial biofilms was imaged by phase-contrast microscopy (Fig. 3*C*). This revealed that the substrate beneath the biofilm contained a series of interconnecting phase-bright trails, which directly correspond to the network of cells that comprised the biofilm before washing except at the leading edge, where faint phase-bright trails can be seen directly in front of vanguard rafts of cells (Fig. 3 *B–D*). This is likely due to the continued forward migration of the rafts during the interval between imaging the intact biofilm and removal of the cells by washing.

Interestingly, we found that the phase-bright trails remain visible despite extensive washing. This suggests that the trails may not be comprised of a "slime" substance. We have noted that scratches in the media are phase-bright in appearance when visualized by phase-contrast microscopy and that *P. aeruginosa* cells that encounter the scratches tend to preferentially migrate along them. We therefore considered the possibility that the trails that develop during *P. aeruginosa* biofilm expansion may be a consequence of physical furrows or grooves in the media that guide cell movement, thereby leading to trail formation.

To determine if the phase-bright trails are physical furrows in the media, we used tapping mode atomic force microscopy (AFM) to analyze the surface topography of the substrate beneath the biofilm, which revealed the presence of numerous furrows that are consistent in dimension with the phase-bright trails observed in the interstitial biofilms (Fig. 3 *E* and *F*, Figs. S5–S8, and *SI Results*). Interestingly, AFM also showed that the furrows under the leading edge rafts are shallower than the trails and are comprised of ramps to the surface of the media (Fig. S7 *A* and *B*, *SI Results*). Phase-contrast imaging of washed biofilms shows that the front edge of the rafts tend to be less visible than the trails (Fig. 3*C*), which is consistent with these being shallower than the trails. These observations suggest that the vanguard rafts migrate over the surface of the media and in the process plow a furrow into the media similar to the action of skis moving across snow.

Our observations suggest that the presence of an extensive furrow system accounts for the manifestation of the intricate trail network in *P. aeruginosa* biofilms as they actively expand over solidified nutrient media. To understand how the interconnected furrow system is forged, we used time-lapse microscopy to examine the process by which cells break out from the furrows to form intersecting trails (Fig. 3*G*, Movie S3). We analyzed the formation of 26 interconnecting trails across seven time-lapse series and observed that interconnecting trails are initiated by small groups comprised of on average 9.4 ± 2.4 cells (minimum, 5; maximum, 15; median, 9) that become longitudinally aligned and oriented perpendicular to the trail. We found that these cells became stationary following realignment. The constant motion of cells in the trail behind this initial cluster results in some cells coming into direct contact with these perpendicular cells and subsequently reorienting so that a second layer of an average of 9.5 ± 2.8 (minimum, 4; maximum, 17; median, 10) longitudinally aligned cells forms behind the initial cluster. Continued migration of cells behind this two-layered cluster results in more cells reorienting with those within the expanding cluster until the supply of cells is sufficient for the newly formed aggregate to commence movement and break away from the trail edge (Fig. 3*G*, Movie S3). When an advancing raft connects with a neighboring raft or trail, the cells from the two paths merge together, resulting in the formation of the extensive trail network (Movie S3). In light of the AFM data, these observations suggest that the coordinated action of an assembled aggregate with a constant supply of cells is required to breach the lip of the furrow to create a new furrow that then intersects with other furrows to form the intricate lattice-like network of trails. Our observations also suggest that a continuous supply of cells to these "bulldozer" aggregates is required to enable them to breach the lip of the furrow and to migrate into virgin territory.

eDNA Facilitates Twitching Motility–Mediated Biofim Expansion. As biofilms of *P. aeruginosa* contain large quantities of eDNA (26–30) and the tfp of *P. aeruginosa* have been shown to bind DNA (31), we explored the possibility that eDNA may also contribute

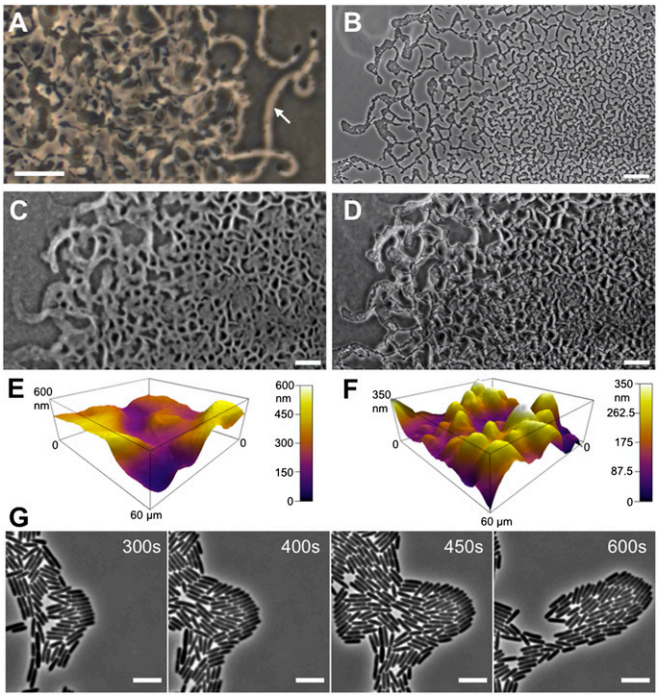

Fig. 3. Interstitial biofilm trails are furrows. (*A*) Phase contrast image of the leading edge of a colony biofilm of wild-type *P. aeruginosa* strain PA103 cultured on LBGG showing the phase-bright trails (white arrow) produced in the wake of the advancing rafts. (Scale bar, 50 µm.) Phase-contrast image of a *P. aeruginosa* PAK interstitial biofilm cultured on TMGG (*B*) and the corresponding phase-contrast image of the underlying substrate showing phase-bright trails (*C*). (*D*) Overlay of *B* and *C*. (Scale bar, 30 µm.) 3D rendered images of AFM measurements taken from washed interstitial biofilm substrate at the leading edge (*E*) and trail network (*F*). (*G*) Phase-contrast images of the assembly of a small bulldozer aggregate breaking away from an established trail in an interstitial biofilm to form a new trail that intersects with another newly formed trail (Movie S3). (Scale bar, 5 µm.) Time indicated taken from the start of the time-series.

to the twitching motility–mediated biofilm expansion. We have found that incorporation of the eDNA degrading enzyme DNaseI into the nutrient media significantly decreased twitching-mediated expansion of *P. aeruginosa* colony biofilms by 76% (*SI Results*, Fig. S4*B*). Fluorescence microscopy of interstitial biofilms cultured in the presence of the eDNA stain TOTO-1 Iodide (TOTO-1, Life Technolgies Corp) revealed that these contain numerous bright punctate foci of eDNA from which tendrils of eDNA emanated, and that beyond these bright foci, eDNA is present at low levels throughout all areas of the interstitial biofilm (Fig. 4 *A*–*E*, *SI Results*, Fig. S4*H*). Time-lapse imaging revealed that as a consequence of cells translocating through areas of high eDNA content, the eDNA becomes redistributed within the biofilm, forming thin tendrils of eDNA radiating from the foci and aligned with the direction of cell migration (Fig. 4*E*, Movie S4). Interestingly, incorporation of DNaseI inhibited the formation of the intricate network of trails (Fig. 1*G*, Fig. S4 *I* and *K*).

To explore the role of eDNA in *P. aeruginosa* biofilm expansion, time-series of interstitial biofilm expansion in the presence of DNaseI were captured at one frame per 2 s. Visual inspection of 1,000-frame time-series showed that in the presence of DNaseI, cells at the leading edge were arranged in vanguard rafts that were similar in appearance to the rafts formed in the absence of DNaseI (Fig. 1*E*, Movie S5). However, in the presence of DNaseI the rafts showed very little outward migration compared with biofilms cultured in the absence of the enzyme (Movie S5). Behind these rafts, cells were arranged haphazardly in broad paths fringed by stationary, laterally aligned cells that are oriented with their major axis perpendicular to the path (Fig. 1*G*, Fig. S4*I*). Cells within the broad paths showed regions of densely packed misaligned cells that appeared to be caught in traffic jams and exhibited little to no movement, whereas in less dense areas individual cells were able to move (Fig. 1*H*, Movie S5).

To better understand the influence of DNaseI on biofilm expansion, cell movements in 100 s of the time-series were tracked (Fig. 1 *F* and *H*) and quantitatively analyzed. These analyses revealed that the presence of DNaseI significantly reduced both the total and net distances translocated by individual cells in the expanding biofilm, compared with biofilms cultured in the absence of the enzyme (Fig. 2 *B* and *C*). In the presence of DNaseI, cells displayed median total and net distances of 2.02 and 0.62 µm within the raft head, 1.96 and 0.46 µm within the raft trails, and 1.60 and 0.29 µm behind the leading edge, respectively (Fig. 2 *B* and *C*). We have further explored the impact of DNaseI on cell movements by comparing net displacements exhibited by the cells as a ratio of the total distance traveled in subgroups of cells separated according to the total distances traveled when cultured in the presence or absence of DNaseI (Fig. S3*B*). These analyses reveal that whereas DNaseI significantly reduces the distances traversed by the majority of cells, there remains a small proportion of cells that can travel considerable total distances. However, the presence of DNaseI significantly reduced the net displacements of these highly motile cells, indicating that these cells often alter their direction of migration. Analyses of time decays of orientation and velocity direction correlations confirm that in the presence of DNaseI, cells tended to frequently change their orientation and direction of travel (Fig. 2*D*, Fig. S2*B*). Interestingly, in the presence of DNaseI, cells in all areas of the biofilm demonstrated very reduced values for both orientational

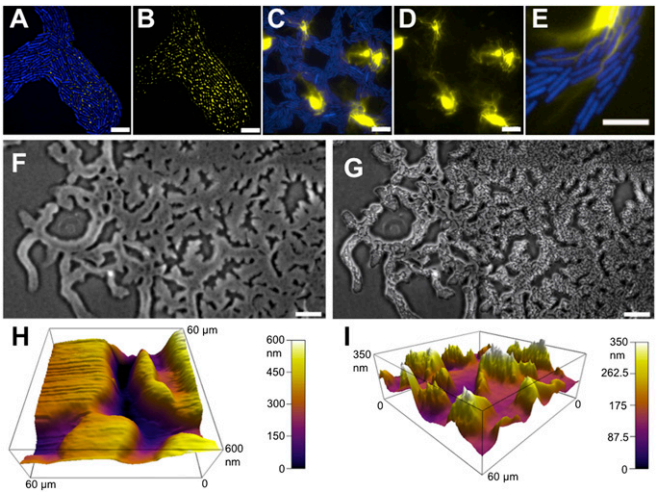

Fig. 4. Interstitial biofilms contain eDNA. Interstitial biofilms of PAK containing pUCP*cfp* (blue) cultured on TMGG containing the eDNA stain TOTO-1 (yellow) and imaged using OMX-Blaze showing eDNA is present in the leading edge rafts (*A* and *B*) and in the trail network (*C* and *D*). *B* and *D* are the TOTO-1 channels of *A* and *C*, respectively. (*E*) Alignment of bacteria and strands of eDNA as it is spread throughout the biofilm by cellular movement. *A* and *B* were obtained with TMGG supplemented with 2 µm TOTO-1, and *C*, *D*, and *E* were obtained with TMGG supplemented with1 µm TOTO-1. The contrast in the TOTO-1 channel was set to enable visualization of low-intensity eDNA staining. (Scale bar, 5 µm.) (*F*) Phase-contrast images of underlying nutrient media that supported an interstitial biofilm of *P. aeruginosa* strain PAK cultured on TMGG in the presence of DNaseI. (*G*) Overlay of the trails depicted in *F* with the corresponding phase-contrast image of the intact interstitial biofilm. (Scale bar, 30 µm.) 3D rendered images of AFM measurements taken from washed interstitial biofilm substrate in the presence of DNaseI at the leading edge (*H*) and behind the leading edge (*I*).

coherence and velocity coherence, indicating that these cells are moving independently of their nearest neighbors (Fig. 2*A*, Fig. S2*A*). These analyses indicate that the presence of DNaseI results in a loss of coordinated behavior during interstitial biofilm migration and that whereas most cells are nonmotile in the presence of DNaseI, those cells that do move tend to move independently of their neighbors and often alter their direction of motion.

To further understand the movements of the population of cells that are capable of migrating large total distances in the presence of DNaseI, the frame-to-frame movement (2-s intervals) of all cells over 100 s was examined. It is evident from these analyses that in the presence of DNaseI ~90% of cells in both the leading edge and behind the leading edge are almost completely stationary, traveling in any given 2 s <0.1 μm (Fig. S3*A*). However, in any 2 s, there is also a small proportion of cells that are capable of traveling up to 1.3 μm (Fig. S3*A*). Interestingly, when the populations of cells that travel at distances >0.6 μm in any 2 s are looked at more closely, it is evident that the distribution of highly motile cells appears quite similar in both the presence and absence of DNaseI (Fig. S3*A*), which suggests that eDNA likely does not necessarily act as a slippery slime to lubricate individual cell movements.

We have often observed in our time-lapse movies of interstitial biofilm expansion that when a raft separates from the biofilm its rate of migration slows, and at times ceases, until it is reconnected with a supply of cells from the biofilm. This suggests that a constant supply of cells to the outer edge of the expanding biofilm is required to maintain movement of the vanguard rafts as they translocate into virgin territory. In the presence of DNaseI, however, the supply of cells to the leading edge rafts from the biofilm is not continuous and can become completely inhibited by traffic jams caused by clusters of misaligned cells (Fig. 1 *E* and *G*, Movie S5). The observed inhibition in the rate of migration of vanguard rafts in the presence of DNaseI may therefore be a consequence of inefficient supply of cells to the leading edge due to traffic jams throughout the biofilm.

In the presence of DNaseI, cells appear to be located within broad tracks edged by laterally aligned cells (Fig. 1*G*). Phase-contrast imaging of washed interstitial biofilms reveals the presence of broad phase-bright tracks that correspond to the populated regions of the biofilm (Fig. 4 *F* and *G*). AFM revealed that inclusion of DNaseI to the media produces broad furrows with high walls that are consistent with the phase-bright tracks (Fig. 4 *H* and *I*, Figs. S5 and S6, *SI Results*). AFM shows that in the presence of DNaseI, rafts are often situated within deep furrows with steep ramps to the surface (Fig. 4*H*, Fig. S7 *C* and *D*, and *SI Results*). Interestingly, we observed that when cells in interstitial biofilms were killed with paraformaldehyde before washing and imaging by AFM, the ramps to the surface were no longer present, and instead it appeared as if the rafts had sunk into the media and were surrounded by steep walls (Fig. S7 *E* and *F*). Our AFM data, taken together with our detailed analyses of cell movements, suggest that eDNA serves to direct traffic flow throughout the furrow network to efficiently supply cells to the leading edge rafts in order for them to attain sufficient speed to skim across the surface and avoid sinking into the semisolid media.

Visual inspection of extended (2,000 s) time-series of interstitial biofilm expansion in the presence of DNaseI reveals that although cells are aligned laterally in fringes at the edges of the paths, groups of longitudinally aligned cells do not assemble behind these lateral edge cells (Movie S5). Thus, eDNA appears to be required for the construction of interconnecting trails by coordinating both the assembly and supply of cells to bulldozer aggregates.

In summary, the inclusion of DNaseI significantly inhibits the traffic flow of cells through the biofilm, characterized by a significant proportion of cells being almost completely stationary at any given time and a lack of coordinated movement of the remaining cells that were capable of some motion. The observed inhibition in the rate of migration of the vanguard rafts in the presence of DNaseI may therefore be a consequence of inefficient supply of cells to the leading edge due to traffic jams throughout the biofilm (Movie S5), which is further exacerbated by the tendency of the slow-moving aggregates to sink into the media rather than skimming across the surface. Thus, it is evident that eDNA is required for coordinating the mass transit of cells through the biofilm for efficient supply of cells into the advancing edge and maintaining collective behaviors, particularly within the vanguard rafts.

Interestingly, interstitial biofilms of nontypeable *Haemophilus influenzae* and *Acinetobacter baumanii* that also actively expand via twitching motility (32, 33) are not associated with the formation of intricate network patterns of trails despite the presence of eDNA in these biofilms (Fig. S9). This suggests that pattern formation by *P. aeruginosa* involves other factors in addition to simply the capacity for twitching motility in the presence of eDNA. Both *H. influenzae* and *A. baumanii* are coccobacilli, whereas *P. aeruginosa* cells are rods; thus, it is possible that cell morphology impacts the tendency toward nematic alignment along the long axis, leading to efficient movement of cells and the emergence of trails. Modeling of *M. xanthus* swarming indicates that the rod morphology of *M. xanthus* cells and regular reversals of movement influence the rate of swarm expansion by reducing the collisional cross-section and enabling escape from collisions and traffic jams (6, 7).

Discussion

Close packing of rod-shaped anisotropic objects leads to nematic order in suspensions of self-propelled particles (active suspensions) (34). However, this alone does not account for the emergence of the intricate network of trails that forms in actively expanding *P. aeruginosa* interstitial biofilms. In this study, the use of sophisticated computer vision and cell tracking along with AFM provided unique insights into the mechanisms that contribute to emergent pattern formation in biological systems. We have identified additional layers of complexity over the basic tendency for nematic alignment in dense collectives of rods. First, there is the formation of the furrow network, which is a pattern more complex than a nematic liquid crystal. Our observations suggest that during interstitial biofilm expansion, the bacteria are tunneling through the interface between the glass substrate and the semisolid media, and it is possible that the observed furrow network is an emergent consequence of the mechanical interactions between the self-propelled nematic liquid crystal pushing against the soft gel, causing it to locally debond from the glass surface. Second, we have found that eDNA appears to be crucial in assembly and coordinating the collective behavior of cells in bulldozer rafts that forge the furrows as well as in preserving the integrity of the network structure once it has been formed. These physical mechanisms coupled with the active nematogenic behavior of rod-shaped bacterial cells lead to the formation of dramatic interconnected network of trails during interstitial biofilm expansion by *P. aeruginosa*.

Our quantitative analyses of the tracking data reveal that eDNA serves to maintain constant traffic flow throughout the trail network by maintaining relative cell alignment. *P. aeruginosa* cells have been shown to spontaneously orient with the direction of extended, concentrated DNA molecules (35). Our time-lapse imaging of interstitial biofilm expansion in the presence of the eDNA stain TOTO-1 revealed that as cells migrated through areas of high eDNA content, they dragged the eDNA along, causing it to be generally aligned with the direction of cell movement (Fig. 4*E*, Movie S4). We propose that this process creates a bed of concentrated, aligned eDNA molecules within the furrow network that helps coordinate collective behaviors by enhancing nematic alignment.

It is evident from our fluorescence microscopy of TOTO-1–stained interstitial biofilms that although eDNA is not homogenously

distributed throughout the biofilm, all areas of the biofilm including the leading edge rafts contain eDNA. Our observations indicate that eDNA is important in coordinating bacterial movements during biofilm expansion and it is clear that inclusion of DNaseI dramatically alters cell behavior and inhibits biofilm expansion. Our analyses revealed that inclusion of DNaseI dramatically affects the behavior of cells predominantly in the leading edge raft heads, causing them to lose coherence with their neighbors. These observations are consistent with a role for eDNA in also mediating intercellular connectivity, thereby enabling the assembly and coordination of cell movements in the large vanguard rafts at the leading edge and in the smaller bulldozer aggregates that forge the interconnected furrow network. Interestingly, tfp binding to the polysaccharide component of surface fibrils is proposed to act like a flexible fishing net that binds cells together in the leading edge rafts of *M. xanthus* cells during S motility–mediated swarming (6). As *P. aeruginosa* tfp bind DNA (31), we propose that tfp–eDNA interactions may serve a similar function in *P. aeruginosa* biofilms by interconnecting cells to one another in a manner similar to the exopolysaccharide fibril net of *M. xanthus*.

In the presence of DNaseI, we observed that cells displayed a lack of collective behavior, resulting in traffic jams of misaligned cells. Interestingly, AFM analysis revealed that the presence of DNaseI resulted in deep, broad furrows with steep inclines to the surface. This suggests that continuous coordinated behavior is required for cells to navigate within the furrow network, providing a constant stream of cells into the advancing rafts to ensure efficient migration of these structures across the surface and the resulting construction of the furrow network. Thus, it is apparent that cellular alignment imposed by eDNA facilitates this mass transit of cells through the furrow network, thereby avoiding traffic jams and ensuring an efficient supply of cells to the migrating front. Our analyses reveal that eDNA also coordinates the movements of cells in the leading edge vanguard rafts and is required for the assembly of cells into the bulldozer aggregates that forge the interconnecting furrows. Our observations have revealed that large-scale self-organization of cells in actively expanding biofilms of *P. aeruginosa* occurs through construction of an intricate network of furrows that is facilitated by eDNA.

Materials and Methods

Biofilm Expansion Assays. Colony biofilms were cultured at 37 °C in humid conditions on 1xLB-Lennox solidified with either 1% agar (Luria Bertani agar, LBA) or 8 g/L gellan gum (Luria Bertani gellan gum, LBGG). Interstitial biofilms were cultured on 0.4xLB-Lennox solidified with 8 g/L gellan gum (twitching motility gellan gum, TMGG). Molten TMGG was poured over sterile slides and solidified at room temperature. Slides were inoculated, covered with a sterile coverslip, and incubated in humid conditions at 37 °C. Media was supplemented with 100 Kunitz units per mL DNaseI (D5025, Sigma Aldrich) or the enzyme storage buffer [50% vol/vol glycerol, 10 mM $MgCl_2$, 10 mM $CaCl_2$, 10 mM Tris·HCl]. To visualize eDNA, TMGG was supplemented with the cell-impermeant DNA stain TOTO-1 (1 or 2 μM; Life Technologies Corp.). For measurement of cell widths by OMX 3D–structured illumination microscopy, TMGG was supplemented with the membrane stain FM1-43FX (5 μg/mL; Life Technologies Corp.)

Segmentation and Tracking of Bacteria. Individual bacteria across 100 s of high-resolution, phase-contrast microscopy time-series captured at one frame per 2 s were identified by segmentation as described previously (23, 24). See *SI Materials and Methods* for description of quantitative analyses used in this study.

AFM. The topography of the media from washed interstitial biofilms was determined using an MFP-3D instrument (Asylum Research). Height images were collected using AC mode in air, with minimized loading force. Antimony (n) doped silicon cantilevers (Veeco TESP-SS) with a nominal spring constant of 42 N/m and a nominal probe curvature radius of 2 nm were used. A scan size of 60 × 60 μm was used, which was large enough to differentiate between different regions of the biofilms. Tapping mode images were processed and analyzed using MFP-3D AFM (Asylum Research) or Image SXM (University of Liverpool) software.

ACKNOWLEDGMENTS. C.B.W. was supported by an Australian National Health and Medical Research Council Senior Research Fellowship (571905). L.T. was supported by a University of Technology Sydney Chancellor's Postdoctoral Fellowship.

1. Donlan RM (2002) Biofilms: Microbial life on surfaces. *Emerg Infect Dis* 8(9):881–890.
2. Donlan RM, Costerton JW (2002) Biofilms: Survival mechanisms of clinically relevant microorganisms. *Clin Microbiol Rev* 15(2):167–193.
3. Sabbuba N, Hughes G, Stickler DJ (2002) The migration of *Proteus mirabilis* and other urinary tract pathogens over Foley catheters. *BJU Int* 89(1):55–60.
4. Mauriello EMF, Mignot T, Yang ZM, Zusman DR (2010) Gliding motility revisited: How do the myxobacteria move without flagella? *Microbiol Mol Biol Rev* 74(2):229–249.
5. Zhang Y, Ducret A, Shaevitz J, Mignot T (2012) From individual cell motility to collective behaviors: Insights from a prokaryote, *Myxococcus xanthus*. *FEMS Microbiol Rev* 36(1):149–164.
6. Wu Y, Jiang Y, Kaiser D, Alber M (2007) Social interactions in myxobacterial swarming. *PLOS Comput Biol* 3(12):e253.
7. Wu Y, Kaiser AD, Jiang Y, Alber MS (2009) Periodic reversal of direction allows Myxobacteria to swarm. *Proc Natl Acad Sci USA* 106(4):1222–1227.
8. Harvey CW, et al. (2011) Study of elastic collisions of *Myxococcus xanthus* in swarms. *Phys Biol* 8(2):026016.
9. Holmes AB, Kalvala S, Whitworth DE (2010) Spatial simulations of myxobacterial development. *PLOS Comput Biol* 6(2):e1000686.
10. Henrichsen J (1983) Twitching motility. *Annu Rev Microbiol* 37(1):81–93.
11. Merz AJ, So M, Sheetz MP (2000) Pilus retraction powers bacterial twitching motility. *Nature* 407(6800):98–102.
12. Skerker JM, Berg HC (2001) Direct observation of extension and retraction of type IV pili. *Proc Natl Acad Sci USA* 98(12):6901–6904.
13. Semmler AB, Whitchurch CB, Mattick JS (1999) A re-examination of twitching motility in *Pseudomonas aeruginosa*. *Microbiology* 145(Pt 10):2863–2873.
14. Vicsek T, Zafeiris A (2012) Collective motion. *Phys Rep* 517(3-4):71–140.
15. Boissard E, Degond P, Motsch S (2013) Trail formation based on directed pheromone deposition. *J Math Biol* 66(6):1267–1301.
16. Levine H, Ben-Jacob E (2004) Physical schemata underlying biological pattern formation-examples, issues and strategies. *Phys Biol* 1(1-2):14–22.
17. Grammaticos B, Badoual M, Aubert M (2007) An (almost) solvable model for bacterial pattern formation. *Physica D* 234(2):90–97.
18. Shapiro JA (1998) Thinking about bacterial populations as multicellular organisms. *Annu Rev Microbiol* 52:81–104.
19. Beatson SA, Whitchurch CB, Semmler AB, Mattick JS (2002) Quorum sensing is not required for twitching motility in *Pseudomonas aeruginosa*. *J Bacteriol* 184(13):3598–3604.
20. Burchard RP (1982) Trail following by gliding bacteria. *J Bacteriol* 152(1):495–501.
21. Stahl SJ, Stewart KR, Williams FD (1983) Extracellular slime associated with *Proteus mirabilis* during swarming. *J Bacteriol* 154(2):930–937.
22. Li YN, et al. (2003) Extracellular polysaccharides mediate pilus retraction during social motility of *Myxococcus xanthus*. *Proc Natl Acad Sci USA* 100(9):5443–5448.
23. Vallotton P, Mililli L, Turnbull L, Whitchurch CB (2010) Segmentation of dense 2D bacilli populations. *International Conference on Digital Image Computing: Techniques and Applications (DICTA)* (IEEE Computer Society, Sydney, Australia), 10.1109/DICTA.2010.23.
24. Vallotton P, et al. (2009) Segmentation and tracking of individual Pseudomonas aeruginosa bacteria in dense populations of motile cells. 24th International Conference Image and Vision Computing New Zealand, 2009 (IEEE Computer Society, Sydney, Australia), 10.1109/IVCNZ.2009.5378409.
25. Kaiser D, Warrick H (2011) *Myxococcus xanthus* swarms are driven by growth and regulated by a pacemaker. *J Bacteriol* 193(21):5898–5904.
26. Murakawa T (1973) Slime production by *Pseudomonas aeruginosa*. IV. Chemical analysis of two varieties of slime produced by *Pseudomonas aeruginosa*. *Jpn J Microbiol* 17(6):513–520.
27. Matsukawa M, Greenberg EP (2004) Putative exopolysaccharide synthesis genes influence *Pseudomonas aeruginosa* biofilm development. *J Bacteriol* 186(14):4449–4456.
28. Steinberger RE, Holden PA (2004) Macromolecular composition of unsaturated *Pseudomonas aeruginosa* biofilms with time and carbon source. *Biofilms* 1(1):37–47.
29. Allesen-Holm M, et al. (2006) A characterization of DNA release in *Pseudomonas aeruginosa* cultures and biofilms. *Mol Microbiol* 59(4):1114–1128.
30. Whitchurch CB, Tolker-Nielsen T, Ragas PC, Mattick JS (2002) Extracellular DNA required for bacterial biofilm formation. *Science* 295(5559):1487.
31. van Schaik EJ, et al. (2005) DNA binding: A novel function of *Pseudomonas aeruginosa* type IV pili. *J Bacteriol* 187(4):1455–1464.
32. Bakaletz LO, et al. (2005) Demonstration of Type IV pilus expression and a twitching phenotype by *Haemophilus influenzae*. *Infect Immun* 73(3):1635–1643.
33. Eijkelkamp BA, et al. (2011) Adherence and motility characteristics of clinical *Acinetobacter baumannii* isolates. *FEMS Microbiol Lett* 323(1):44–51.
34. Narayan V, Menon N, Ramaswamy S (2006) Nonequilibrium steady states in a vibrated-rod monolayer: tetratic, nematic, and smectic correlations. *J Stat Mech* P01005.
35. Smalyukh II, Butler J, Shrout JD, Parsek MR, Wong GC (2008) Elasticity-mediated nematiclike bacterial organization in model extracellular DNA matrix. *Phys Rev E Stat Nonlin Soft Matter Phys* 78(3 Pt 1):030701.